Optimizing Adaptive Coding and Modulation for Satellite Network with ML-based CSI Prediction

Xinmu Wang*†‡, Hewu Li†‡, Qian Wu†‡§
*Graduate School at Shenzhen, Tsinghua University, Shenzhen 518055, China
†Institute for Network Sciences and Cyberspace, Tsinghua University, Beijing 100084, China
‡Beijing National Research Center for Information Science and Technology (Tsinghua University), Beijing 100084, China
wangxm16@mails.tsinghua.edu.cn, {lihewu, wuqian}@cernet.edu.cn, §Corresponding author

***Abstract*—The introduction of adaptive coding and modulation (ACM) in DVB-S2 improves system capacity. Transmission mode is adapted to receiving conditions which are fed back through return link supported in DVB-RCS2. A big challenge is that ACM scheme has to follow channel variations which are faster than the delay between channel measurement and feedback reception. Channel state information (CSI) for next transmission often differs profoundly from current estimated result. This causes the mismatch between transmission mode and channel quality. To resolve this problem, this paper deploys a CSI prediction framework and implements machine learning (ML) algorithms for accuracy. Compared with conventional prediction algorithms, ML algorithms have advantage on handling the complicate and changeable time series. In ACM scheme, MODCOD selection is based on channel SNR and MODCOD SNR threshold. Therefore, this prediction work takes channel SNR for next transmission as the prediction target and past SNR plus other correlated information as the prediction basis. To verify prediction accuracy, this paper discusses major factors impacting channel situation in detail and proposes a synthesis channel fading model. Numerical experiment results demonstrate the improvement on system performance while the efficiency and complexity of different commonly-used ML algorithms are also included.**

***Index Terms*—ACM, MODCOD, CSI, machine learning, SNR**

I. Introduction

With global coverage, satellite communication can provide Internet access for regions lacking in terrestrial network infrastructure or passengers traveling on airplanes and trains [3]. But satellite-ground link, known as the last mile connection, always becomes the bottleneck for network throughput. Traditional worst-case design, constant coding and modulation (CCM), fails to efficiently utilize radio resources. Instead, adaptive coding and modulation (ACM) is a promising fading mitigation technique [4]. ACM allows transmission parameters to dynamically adapt to channel signal-to-noise ratio (SNR). Sending terminal selects transmission mode based on feedback signaling. Receiving terminal can inform sending terminal either CSI (*e.g.* SNR, RSSI, Rice factor, Doppler frequency, BER/PER/FER, [5] etc.) or the identifier of MODCOD through return link.

The changeability of satellite channel and the long-time delay represent a significant challenge for an ACM scheme to follow the channel variations. In satellite networks, round-trip time (RTT) and inherit latency take over 500ms [6]. While severe rain attenuation, plus shadowing effects can cause a short-term channel fading exceeding 10 or even 20 dB at Ka band frequencies with a decay rate of 0.5 to 1dB/s. For a LEO-ground link, free space loss varies in a scope of nearly 10 dB from perigee to apogee according to propagation length. Thus, CSI for next transmission will differ profoundly from the current measurement result. Besides, measurement error of CSI is unavoidable, *e.g.* DA-SNORE channel SNR estimation algorithm has 0.2dB error standard deviation [7].

An ACM scheme assuming a simple channel fading model may perform well on smooth channel conditions with stable channel states and only a few state transitions. However, for complicate channel fading situations, such schemes' performance is unacceptable. Generally, a satellite communication system requires 99% physical layer availability [8]. To guarantee the aforementioned goal, a safety margin should be set in case of overestimated channel SNR. But for other cases MODCOD with lower spectral efficiency may be chosen, and thus remaining notable unutilized bandwidth redundancy. The SNR threshold gap between two adjacent MODCODs is approximately 2dB while the disparity between their spectral efficiency ranges from 0.4 to 0.5 Mbit/s/Hz. For 4.35MHz bandwidth in an iridium satellite channel, this will lead to a difference of nearly 2Mbit/s link throughput. If the mismatch between channel SNR and the MODCOD SNR threshold spans over the adjacent MODCODs, system performance will be much worse. Fig. 1 shows an actual operation of a conventional ACM scheme. During the communication period, the worst case with 4.5dB SNR redundancy in a fluctuating channel situation causes over 4Mbit/s link throughput loss.

Therefore, this paper introduces ML-based CSI prediction to ACM scheme. Motivated by the success of ML on similar tasks *e.g.* video bitrate adaption, this paper tries to use ML-based methods to deal with the CSI variation. The long-time-delay changeable information sequences is handled by the prediction framework. Channel SNR for next transmission is chosen as prediction target since MODCOD selection is based on the match of SNR threshold. Past CSI (including SNR and other correlated information, *e.g.* propagation delay, environment shadowing state and rain attenuation state) is taken as a multi-dimension prediction basis. This paper comprehensively analyzes accuracy and cost of different ML algorithms, compares

978-1-5386-7646-2/19/$31.00 ©2019 IEEE

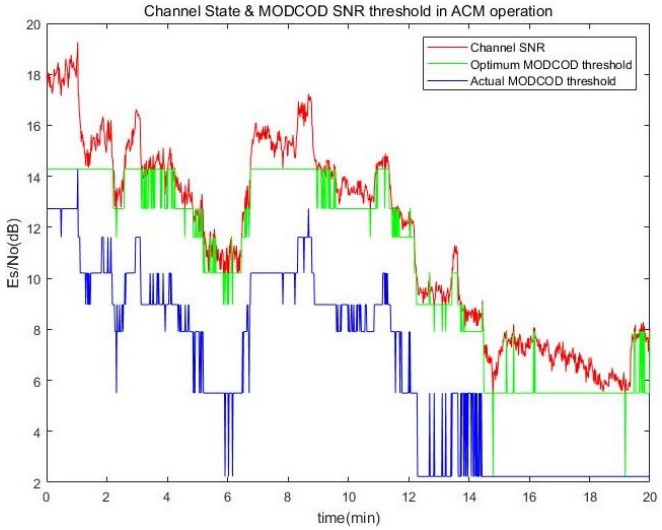

Fig. 1: Channel SNR and MODCOD threshold

system performance with conventional ACM MODCOD selection. The efficiency and feasibility of ML-based methods are also concluded. Lightweight ML algorithms are preferred due to the ability of generalization and less overhead for online-training. A tradeoff between performance and complexity is further discussed.

II. System Model

A. Satellite ACM System Architecture

The transparent satellite architecture (classical amplify and forward) is shown in Fig. 2 [7]. It is composed by Gateway (GW) (containing an ACM DVB-S2 modulator), Satellite, and Satellite receiving Terminal (ST) connected to GW via return channel. For regenerative satellite architecture with on-board ACM processing and switching, the case is approximate. This paper considers transparent satellite system for more complexity brought by apparently longer end-to-end delay. Satellite forwarding link is based on DVB-S2 [1] and return link is based on DVB-RCS2 [2]. The source rate control may

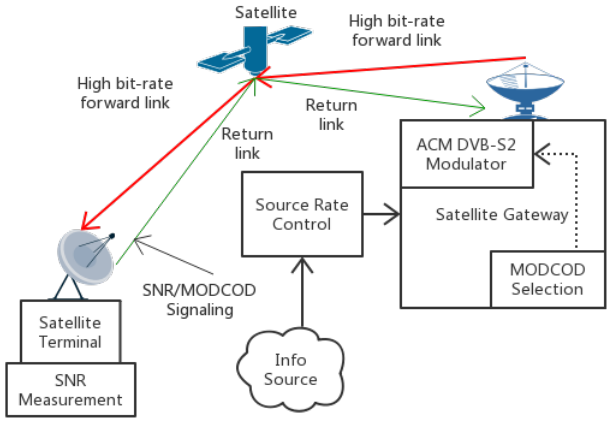

Fig. 2: System Architecture

Table 1 28 MODCODs supported in DVB-S2.

MODCOD	Spectral Efficiency	Ideal Es/No
QPSK,1/4	**0.490243 bit/s/Hz**	**-2.35 dB**
QPSK,1/3	0.656448 bit/s/Hz	-1.24 dB
QPSK,2/5	0.789412 bit/s/Hz	-0.30 dB
QPSK,1/2	0.988858 bit/s/Hz	1.00dB
QPSK,3/5	**1.188304 bit/s/Hz**	**2.23 dB**
QPSK,2/3	1.322253 bit/s/Hz	3.10dB
QPSK,3/4	1.487473 bit/s/Hz	4.03 dB
QPSK,4/5	1.587196 bit/s/Hz	4.68 dB
QPSK,5/6	1.654663 bit/s/Hz	5.18 dB
QPSK,8/9	1.766451 bit/s/Hz	6.20 dB
QPSK,9/10	1.788612 bit/s/Hz	6.42 dB
8PSK,3/5	**1.779991 bit/s/Hz**	**5.50 dB**
8PSK,2/3	1.980636 bit/s/Hz	6.62 dB
8PSK,3/4	**2.228124 bit/s/Hz**	**7.91 dB**
8PSK,5/6	2.478562 bit/s/Hz	9.35 dB
8PSK,8/9	2.646012 bit/s/Hz	10.69 dB
8PSK,9/10	2.679207 bit/s/Hz	10.98 dB
16APSK,2/3	**2.637201 bit/s/Hz**	**8.97 dB**
16APSK,3/4	**2.966728 bit/s/Hz**	**10.21 dB**
16APSK,5/6	**3.300184 bit/s/Hz**	**11.61 dB**
16APSK,8/9	3.523143 bit/s/Hz	12.89 dB
16APSK,9/10	3.567342 bit/s/Hz	13.13 dB
32APSK,3/4	**3.703295 bit/s/Hz**	**12.73 dB**
32APSK,4/5	3.951571 bit/s/Hz	13.64 dB
32APSK,5/6	**4.119540 bit/s/Hz**	**14.28 dB**
32APSK,8/9	4.397854 bit/s/Hz	15.69 dB
32APSK,9/10	4.453027 bit/s/Hz	16.05 dB

be directly applied to the source(s) or locally at the gateway input or via network traffic control in case of information overflow during severe channel fadings.

Since the downlink carrier bandwidth is assumed constant, DVB-S2 ACM modulator operates at a constant symbol rate. Each physical layer frame transports a coded block and adopts a uniform modulation format. When ACM scheme is deployed, coding rate and modulation level may change frame-by-frame. Satellite terminal generates a signaling containing the channel SNR or the most efficient MODCOD the satellite terminal can decode based on the collected CSI measurement results. Then the signaling information is provided to the satellite gateway via the return link. In case of increasing signaling overhead on the return link, satellite terminal only sends a message when the variations of channel conditions imply a change on the spectral efficiency instead of periodical reports.

The feedbacks of satellite terminals are considered by the gateway in coding and modulating the data packets. During severe channel fadings, *e.g.* heavy rain attenuation, information rate is reduced while forward error correction (FEC) redundancy or modulation ruggedness is increased at the same time. While for the clear sky cases a higher information rate is delivered to the satellite terminals since a higher physical layer transmission mode can be decoded.

B. ACM MODCOD Subset

DVB-S2 supports 28 MODCODs listed in Table 1, and the ideal SNR thresholds are based on $BER = 10^{-7}$. SNR threshold gap between two adjacent MODCODs also makes for avoiding frequent switch. In practice, a carefully selected MODCOD subset is able to get system performance close to the optimum, with much lower equipment burden [14].

The subset optimization has been studied in [14] and [20] aiming to maximize the system capacity which the candidate MODCODs can provide. Selected MODCODs are marked in Table 1. To guarantee the 99% physical layer availability, the lowest MODCOD **QPSK,1/4** should be kept in any cases. $M = \{M_1, M_2, ..., M_K\}$ denotes the MODCOD subset, and the unit M_i in this set is chosen from Table 1 with spectral efficiency SE_i and SNR Threshold TH_i. K is the subset size generally fewer than 10. $S = \{SNR_1, SNR_2, ..., SNR_T\}$ denotes the channel SNR during the communication period with duration T. The subset selection is performed with solving the problem mathematically described as:

$$\prod = \arg\max \sum_{t=0}^{T} \sum_{i=0}^{K} SE_i \cdot x_{i,t} \tag{1}$$

$$x_{i,t} = \begin{cases} 1, & TH_i \leq SNR_t \leq TH_{i+1} \\ 1, & TH_K \leq SNR_t \\ 0, & \text{Otherwise} \end{cases} \tag{2}$$

III. CHANNEL FADING MODEL

A. Channel Fading Factors

Major channel fading factors are gaseous absorption, cloud attenuation, melting layer attenuation, tropospheric scintillation, low-angle fading, multipath fading and signal shadowing. For Ka band fixed satellite communication, channel characteristics are mainly affected by rain attenuation and other tropospheric effects [9]. For mobile cases, multipath fading and shadowing also need to be considered since land mobile satellite (LMS) terminals often operate under cluttered circumstances [10] (urban, tree-shadowed areas, etc.) where shadowing effects dominate. Generally, signal envelope and phase of fixed satellite communication channel are approximately modeled as Gaussian. For land mobile satellite communications channel, signal envelope is modeled as shadowed Rician while signal phase is modeled as Gaussian [11].

B. Channel Simulation

Simulation is based on LMS channel in terms of LEO communication. This case provides more complex conditions where both weather and shadowing effects are considered. Channel state transitions and durations are usually modeled as first-order Markov (state duration depends on a transition probability matrix) or more flexible semi-Markov process (state duration follows an exponential distributions) [12]. Fig. 3 (a) and Fig. 3 (b) illustrate a typical 3-state model. This simulation defines a 3-state model [10], [12], from line-of-sight (LOS) to deep shadow for shadowing effects and a 4-state model [13], from clean sky to heavy rain for weather. Both use first-order Markov chain. Transition probability for a Markov chain can be symbolized by an $M \times M$ matrix P, $M = 3$ for shadow state and $M = 4$ for weather state, where $p_{ij} = P(S_{(t+1)} = j | S_t = i)$ and fulfill the equation $\sum_{j=1}^{M} p_{ij} = 1$. Investigation results show that attenuation level A of each state is almost linear relationship with slope of one, with a deviation σ_A [13]. Parameters for the simulation model described above are extracted mainly from measurement results in [10] and [11], and may vary for different scenarios.

The signal model is given by

$$y_k = \sqrt{\gamma} \cdot h_k s_k + w_k \tag{3}$$

with y_k the symbol received at the k-th time instant, s_k the transmitted symbol, h_k the channel coefficient and γ representing the channel SNR; accordingly, w_k comprises the interference and unit-power noise contribution.

The signal-to-noise ratio (SNR) for receiver i is described as:

$$\gamma_i = EIRP_i + (G - T)_i - L_i - K - B. \tag{4}$$

where $EIRP$ is the effective isotropic radiated power, $(G-T)$ is the figure of merit, L is the path loss, K is the logarithmic value of the Boltzmann constant, and B denotes the logarithmic value of the downlink spectrum bandwidth.

With transmitted power and other factors (*e.g.* signal bandwidth, receiving-antenna gain, etc.) held constant, Channel SNR's variation rests on free space loss (calculated by transmission distance) and propagation medium loss (mainly determined by weather and environment states). Besides SNR, simulation data also include propagation delay (RTT/2), terminal velocity, weather and environment state for each communication period lasting 20 minutes (visible time for LEO-ground link is assumed as 20 minutes). Channel situation samples for several simulation periods are shown in Fig. 4 and change curve of channel SNR is depicted. In these samples, the satellite moves from its apogee to perigee and then from perigee to apogee, coming with free space attenuation down and then rise; channel SNR undergoes several rapid jumps as land mobile terminal experiences shadow effects to different degrees; severe rain attenuation can cause a huge decay on channel quality. Major impactors on channel fading are concerned in simulation and this scenario provide enough complicacy for verifying ACM performance achieved in the following work. Simulation system parameters considered are:

- Satellite Orbit: LEO
- Band: Ka
- Duplexing: FDD
- Forward Link Frequency: 22.5GHz
- Reverse Link Frequency: 23.5GHz
- Channel: LMS
- Elevation: $20^\circ \sim 80^\circ$
- DVB-S2 Codeword Length: 16200 [1]
- DVB-RCS2 Burst Length: 540 [2]

IV. MODCOD SELECTION & CSI PREDICTION

A. MODCOD Selection Procedure

MODCOD selection is derived from the matching between SNR prediction result and MODCOD thresholds looked up in MODCOD subset. Hysteresis is sometimes included in case of ping-pong between consecutive MODCODs. In practice the mapping between channel SNR prediction results and actual channel conditions may not be well-matched due

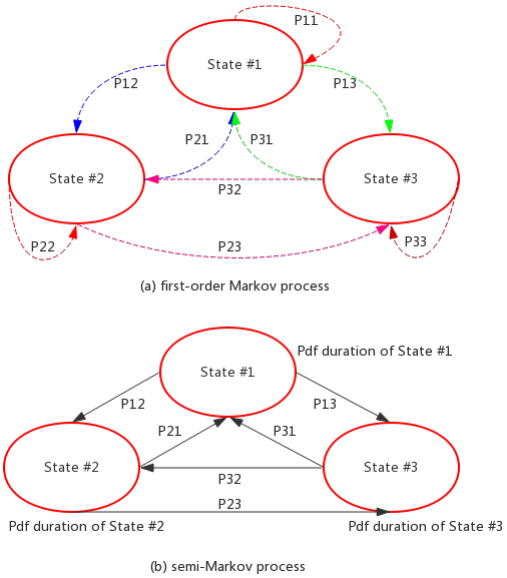

Fig. 3: Channel state transition

to the channel variations mentioned above. Therefore, SNR prediction results cannot be directly used for the selection procedure and a safety margin should be adopted. To guarantee the 99% physical layer availability, the safety margin has to cover the SNR prediction and measurement deviation in 99% of cases. For simplicity, the margin can be denoted as $\Delta SNR_{Margin} = \Delta SNR_{prediction} + \Delta SNR_{measurement}$. When a SNR prediction result $SNR_{prediction}$ is obtained, the SNR threshold of each MODCOD is compared with $SNR_{prediction} + \Delta SNR_{Margin}$. If a MODCOD has the highest spectral efficiency and its SNR threshold satisfies $SNR_{threshold} \leq SNR_{prediction} + \Delta SNR_{Margin}$, then this MODCOD is the optimal choice. Under certain circumstance, no MODCOD can be chosen and then communication is unavailable, and such cases should be no more than 1%. As the deviation of DA-SNORE algorithm is 0.2dB, $\Delta SNR_{measurement}$ is set as 0.2dB in the numerical experiment and the major component of safety margin is resulted from $\Delta SNR_{prediction}$.

B. Prediction Framework

Statistics reveal a portion of CSI variation rules. Satellite has fixed orbit and determined transmission path with land terminals. Distributions of fading factors in the same area covered by a satellite always coincide. Cyclic characters of satellite motion provide similar scenarios for communications in certain periods. While insufficient and crude samples fail to elicit a rigorous discipline, obstructing the utilization of known regulations since it is impossible to draw a formula directly from raw data. However, ML can work through this predicament by optimizing a performance criterion based on past experience. It uses statistical techniques to give computer system the ability of progressively learning with data from a specific task other than explicitly programming [15]. Fig. 5 illustrates how a ML-based prediction model is applied to MODCOD selection procedure in ACM scheme, making a difference that use ML-based prediction results other than the value of last turn. On contrast against the incapability of a fix rule or simple coarse-grain model, ML algorithms are expected to be optimum approaches for prediction task. Prior prediction methods, *e.g.* weighted arithmetic or harmonic mean, and auto-regression [16], all fall in short of applicability and generality when coping with information sequences fluctuating over time and across environment. But recent applications of ML-based methods on similar tasks have already proved to be success, *e.g.* adaptive video bitrate based on network throughput prediction [17], [18].

The prediction framework takes channel SNR for next transmission as CSI prediction output. The input includes five types of information sequences (k previous turns of SNR, propagation delay, terminal velocity, weather and environment state, k set as 20 in experiment). After the measurement result of SNR_t is obtained, ML-based prediction model adjusts its parameters or structure according to prediction deviation $\Delta SNR_t = Predict(SNR_t) - Real(SNR_t)$. Channel variation's real-time sensitivity requires on-line training, and immediate modification help to overcome overfitting [19]. X denotes the set of all CSI values taken by measurement, and $Y = [-4, 20]$ dB represents SNR range. This model uses past sequence of CSI to obtain a predictive function f of SNR for next transmission, and thus function f has to minimize the following objective:

$$\theta = \arg\min \int_{X \times Y} \|f(x) - y\| \, d\rho \tag{5}$$

ρ is a probability measure on $X \times Y$, and f approximates the mapping from X to Y.

C. Results and Analysis

Different ML algorithms, *e.g.* k-Nearest Neighbors (kNN), Gradient Boosting Regression Tree (GBRT), Multi-layer Perceptron (MLP), etc. are evaluated by offline experiment performed on Intel i5-2.2GHz, 4GB RAM, Windows 10. Simulation produced 1000 samples (900 for training and 100 for test) and each sample contains 1200 turns of CSI. SVR (support vector regression) fails to complete training in a tolerant timeout, and thus this method is not included. Mean absolute error (MAE) (more suitable than mean squared error, MSE), training time overhead and the average ratio of optimal match between SNR prediction result and MODCOD threshold (selected MODCOD has the highest spectral efficiency and can be decoded) are listed in Table 3. Since prediction accuracy alone cannot directly demonstrates system performance, safety margin, available capacity and utilization of the optimal capacity for ACM scheme implemented with different ML algorithms are listed in Table 4. Safety margin used for the match process equals SNR measurement standard deviation 0.2dB [7] plus SNR redundancy kept for prediction inaccuracy. SNR redundancy has to cover prediction deviation in 99% cases (communication turns with top 1% SNR prediction deviation are unreliable and this part of capacity is abandoned due

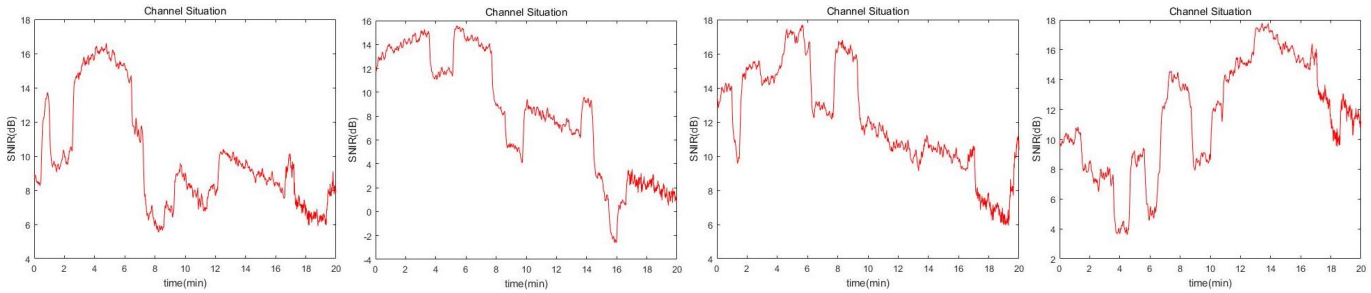

(a) (b) (c) (d)

Fig. 4: Channel SNR simulation samples.

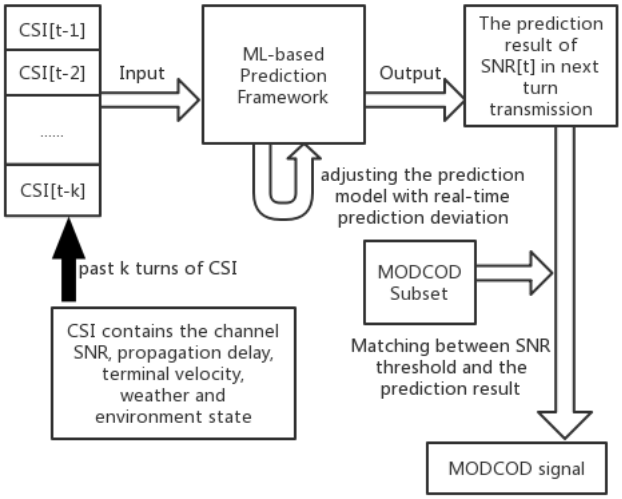

Fig. 5: CSI prediction and MODCOD selection

Table 3 Prediction Accuracy and Cost.

Method	MAE	Time	Optimal match ratio
MLP	0.272	1001.8s	30%
Linear Regression	0.271	17.1s	29.2%
Random Forest	0.275	1482.6s	29%
GBRT	0.274	965.4s	28.3%
Bagging	0.283	766.2s	28.1%
AdaBoost	0.382	868.4s	25%
Decision Tree	0.392	121.3s	17.5%
Extra Tree	0.395	37.2s	16.7%
kNN	0.417	251.2s	13.8%
Baseline	**0.419**	**-**	**13.04%**

to unacceptable bit error rate). System capacity is calculated according to 4.35MHz channel bandwidth.

Baseline using last turn SNR shows a safety margin of 1.99 dB has to be kept, and achieves 13.04% **optimal match ratio and 12723Mbit average capacity**, while weighted mean proves to be even worse. **The optimal system capacity is 16368Mbit**. Experiment illustrates notable prediction accuracy of most ML algorithms and acceptable time overhead for such scale (1000×1200) data set. Thus, on-line training is feasible. Large promotion space still exists since ML methods are test on unfiltered raw data without complex tuning but using universal models. Comparison between different ML

Table 4 SNR safety margin and System Capacity.

Method	Safety margin	Capacity	Utilization Ratio
MLP	1.29 dB	14109Mbit	86.2%
Linear Regression	1.30 dB	14084Mbit	86%
Random Forest	1.30 dB	14072Mbit	85.9%
GBRT	1.31 dB	14069Mbit	85.9%
Bagging	1.31 dB	13859Mbit	84.7%
AdaBoost	1.43 dB	13799Mbit	84.3%
Decision Tree	1.71 dB	13592Mbit	83%
Extra Tree	1.76 dB	13079Mbit	79.9%
kNN	1.95 dB	12905Mbit	78.8%
Baseline	**1.99 dB**	**12723Mbit**	**77.7%**

algorithms also show that a complex algorithm, such as MLP, though achieve the best performance, takes much more time. In this experiment, MLP can be further tuned by enlarging hidden layer size (set as 1 layer with 100 neurons in this experiment) for higher score, but the price of overhead and damage on generalization ability need a tradeoff; rectified linear unit function (RELU) is proved to be superior than other activation function and quasi-Newton methods performs much better than stochastic gradient descent on weight optimization. Linear regression, an obviously simple algorithm, achieves nearly as high score as MLP, with the lowest time overhead, which means a simple method can be powerful and should be the first choice on this kind of task.

Prediction work uses a multi-angle basis containing 5 types of information sequences other than past channel SNR solely as a single variable, and taking correlated information from more aspects as model input proves to be superior on prediction accuracy and a help to enhance ML model's learning efficiency. Moreover, the number of CSI turns (set as 20 in this experiment) input in ML model has to be weighed and balanced. Too few turns of CSI fail to train ML model to learn the changing rules or variation tendency of channel SNR; on the other hand, CSI long time ago has quite weak association with current or immediate future case, and excessive irrelevant input variables only increase storage and calculation burden.

System performance enhancement comes from two aspects: accurate CSI prediction lowers safety margin, coming with less redundancy; avoidance on SNR underestimation also raises radio resource utilization. For a prerequisite of 99% physical layer availability, ML-based CSI prediction model

brings an average increase of capacity up to 10.9%, with acceptable overhead. This improvement varies in different data set, and further modification on ML model need support of more realistic simulation work in case of overfitting within a single scenario. In practical application, a ML model need offline training through recorded data before deployment, and then continuously iterates or modifies according to real-time operation aiming for full advantage of both historical laws and transient rules.

V. Conclusion

This paper focuses on implementing ML algorithms to CSI prediction in satellite network and using the enhanced prediction results to optimize system capacity. By testing different ML algorithms, the improvement on system performance and the feasibility of deploying a ML-based prediction frame work are demonstrated. As illustrated in the experiment, a simple method can achieve high score on this kind of task with much less overhead, and has lower probability of overfitting compared with complex models. Thus, in on-line training work, lightweight algorithms are preferred. Considering the limitation of using past channel SNR solely for prediction work, this experiment adds other four correlated information sequences providing a multi-dimension prediction basis. The learning efficiency of a ML model relies on what kinds of CSI introduced as model input. Closely associated variables are great help to convey changing rules and variation trend of channel SNR but others may prove to be obstacles on model adjustment and an increase on storage or calculation burden. Model input also need a weigh on the number of CSI turns (set as 20 for the best performance in this experiment), and this has to be verified whether a change for different scenarios is needed according to operation experience.

In many cases, the drastic changes of channel conditions may disable the CSI prediction framework in MODCOD selection, and the optimal MODCOD needs to be selected based on both the CSIs as well as the ACKs/NACKs. Safety margin also need adjustment in line with prediction accuracy, and this will be different for open loop CSI (timely but inaccurate) and closed loop CSI (accurate but delayed). Model update and safety margin alteration in previous work are performed through an off-line training and remain unchanged during communication operation. Real-time adjustment demands cautiously decision expected to be fulfilled by a reinforcement learning framework studied in the future work. Moreover, land terminals in adjacent areas share almost the same channel condition, which means ML-based CSI prediction model can apply prediction results obtained from one terminal to a cluster, and less calculation and storage resources are needed.

Acknowledgment

This work is supported by National Natural Science Foundation of China (91738202), Beijing Municipal Science Technology Commission (Z171100005217001), and Beijing National Research Center for Information Science and Technology (20031887521).

References

[1] Digital Video Broadcasting (DVB); Second Generation Framing Structure, Channel Coding and Modulation Systems for Broadcasting, Interactive Services, News Gathering and Other Broad-Band Satellite Applications (DVB-S2), European Broadcasting Union (EBU), ETSI EN 302 307-1 V1.4.1, Nov. 2014.

[2] Second Generation DVB Interactive Satellite System (DVB-RCS2); Part 2: Lower Layers for Satellite standard, ETSI EN 30 301 545-2 V1.2.1 (2014-04)

[3] S. Cioni, R.D. Gaudenzi, and R. Rinaldo, "Channel estimation and physical layer adaptation techniques for satellite networks exploiting adaptive coding and modulation", International Journal of Satellite Communications and Networking, vol. 26, no. 2, pp. 157–188, Mar./Apr. 2008.

[4] T. Javornik, M. Mohorčič, A. Švigelj,et al, "Adaptive Coding and Modulation for Mobile Wireless Access via High Altitude Platforms", Wireless Personal Communications (2005) 32: 301-317.

[5] D. Tarchi, G.E. Corazza, A. Vanelli-Coralli, "Adaptive coding and modulation techniques for mobile satellite communications: A state estimation approach", Advanced Satellite Multimedia Systems Conference (ASMS) and 12th Signal Processing for Space Communications Workshop (SPSC), 2012 6th

[6] Joon-Gyu Ryu, Deock-Gil Oh, Hyun-Ho Kim, et al, "Proposal of an Algorithm for an Efficient Forward Link Adaptive Coding and Modulation System for Satellite Communication", Journal of Electromagnetic Engineering and Science, vol.16, 80-86, APR. 2016.

[7] R. Rinaldo, M.A. Vazquez-Castro, and A. Morello, "DVB-S2 ACM modes for IP and MPEG unicast applications", International Journal of Satellite Communications and Networking, vol.22, 2004.

[8] E. Alberty, S. Defever, C. Moreau, et al, "Adaptive coding and modulation for the DVB-S2 standard interactive applications: Capacity assessment and key system issues", IEEE Wireless Communications, vol.14, 2007.

[9] A. Dissanayake, J. Allnutt, and F. Haidara, "A Prediction Model that Combines Rain Attenuation and Other Propagation Impairments Along Earth- Satellite Paths", Online Journal of Space Communication, vol.45, 1546-1558, 1997.

[10] F. P. Fontán, M. Vázquez-Castro, C.E. Cabado, et al, "Statistical modeling of the LMS channel", IEEE Transaction on Vehicular Technology, vol.50, no.6, NOV. 2001.

[11] C. Loo, "Statistical models for land mobile and fixed satellite communications at Ka band", Proceedings of Vehicular Technology Conference, vol.2, issue.46, 1023-1027, 1996.

[12] F. P. Fontan, "Channel Modeling for Land Mobile Satellite Services", Proceedings of the Fourth European Conference on Antennas and Propagation, 1-5, 2010.

[13] M. Zhang, S. Kim, et al, "A Statistical Approach for Dynamic Rain Attenuation Model" AIAA International Communications Satellite Systems Conference, 2011.

[14] V. Boussemart, H. Brandt and M. Berioli, "Subset Optimization of Adaptive Coding and Modulation Schemes for Broadband Satellite Systems", IEEE International Conference on Communications, 2010.

[15] Samuel Arthur, "Some Studies in Machine Learning Using the Game of Checkers", IBM Journal of Research and Development, vol 3, 1959, pp 210-229.

[16] Q. He, C. Dovrolis, and M. Ammar. "On the Predictability of Large Transfer TCP Throughput", In Proc. ACM SIGCOMM, 2005.

[17] Y. Sun, X. Yin, J, Jiang, et al, "CS2P: Improving Video Bitrate Selection and Adaptation with Data-Driven Throughput Prediction" In Proc. ACM SIGCOMM, 2016.

[18] H. Mao, R. Netravali, and M. Alizadeh, "Neural Adaptive Video Streaming with Pensieve", In Proc. ACM SIGCOMM, 2017.

[19] S.Yun and C.Caramanis, "Reinforcement learning for link adaptation in MIMO-OFDM wireless systems", GLOBECOM - IEEE Global Telecommunications Conference, 2010.

[20] M. Smolnikar, A. Aroumont, M. Mohorcic, T. Javornik, and L. Castanet, "On transmission modes subset selection in DVB-S2/RCS satellite systems," 2008 International Workshop on Satellite and Space Communications, IWSSC'08, Conference Proceedings, pp. 263—267. https://doi.org/10.1109/IWSSC.2008.4656808